

Diffusive behavior of states in the Hubbard-Stratonovitch transformation

S. Fahy and D. R. Hamann

AT&T Bell Laboratories, Murray Hill, New Jersey 07974

(Received 22 January 1990; revised manuscript received 24 July 1990)

The Hubbard-Stratonovitch auxiliary-field approach to projection of the ground state of an interacting fermion system from a trial state is examined. It is shown that the method is equivalent to solving a differential equation with diffusion, drift, and branching terms on the manifold of normalized Slater determinants. Explicit general expressions are given for the coefficients of the diffusion equation in terms of the Hubbard-Stratonovitch fields. The form of the equation is somewhat similar to that obtained in the continuum Green's-function Monte Carlo method, although its interpretation and relation to the physical many-body problem is quite different. The character of the representation of the many-body ground state arising in the auxiliary-field projection approach is discussed within this framework. The diffusion process is normally found to concentrate the states representing the ground state near the classical mean-field solutions. The consequences of this picture of the auxiliary-field approach for the "fermion minus-sign" problem in this context are discussed, and some conclusions are reached concerning the range of validity of a recently suggested approximation where minus signs are ignored.

I. INTRODUCTION

The idea of projecting out the ground-state wave function of a quantum-mechanical system by evolution from a trial wave function Ψ_t according to Schrödinger's equation in imaginary time is an old one.¹ The exponential decay of the amplitude of higher-energy states in the imaginary-time evolution

$$\begin{aligned} \lim_{\beta \rightarrow \infty} \exp(-\beta H) |\Psi_t\rangle &= \lim_{\beta \rightarrow \infty} \sum_i \exp(-\beta \epsilon_i) |\Psi_i\rangle \langle \Psi_i | \Psi_t \rangle \\ &= \exp(-\beta \epsilon_0) |\Psi_0\rangle \langle \Psi_0 | \Psi_t \rangle \end{aligned} \quad (1)$$

leaves only the lowest state Ψ_0 which is not orthogonal to the trial-state Ψ_t in the infinite- β limit. As a method of calculating the ground-state properties of interacting many-body systems, this projection approach has been very fruitful. In the Monte Carlo simulation of the imaginary time evolution, two techniques have principally been used, viz., the Green's-function or diffusion Monte Carlo approach,²⁻⁶ and, more recently, the auxiliary-field approach.⁷⁻¹¹ The essential difference between the two methods is the manner in which the propagator $\exp(-\beta H)$ is evaluated. As we will see, the way we represent the propagator directly determines, in turn, how the resulting ground state will be represented. Indeed, while it is true that the many-body state follows the same propagation in any exact representation of the propagator, different ways of realizing the propagation will give rise to very different representations of the propagated many-body state. The specific nature of the representation determines how we ultimately evaluate the expectation values of physical quantities of interest.

The purpose of this work is to understand some aspects of the representation that arises in the auxiliary-field method as it has been applied to the imaginary-time projection of fermion ground states of discrete lattice mod-

els. Our principal result is the demonstration that a weight function which arises in this representation obeys a diffusion equation. We can then exploit our general knowledge of the qualitative behavior of diffusion equations to obtain information about the character of that representation of many-body states which is built into the auxiliary-field approach.

Although the diffusion Monte Carlo approach to continuum interacting fermion systems and the auxiliary-field approach to fermions on a lattice appear to have a very tenuous relationship with one another, our result reveals a surprising formal analogy between the two problems. We emphasize at the outset that this is a formal analogy only, that very important differences remain between the two approaches, and that care must be exercised in invoking the analogy. This is especially true in considering the relationship between the formal representation and the original physical many-body problem. For example, we will see that the "fermion sign problems" as they occur in these two different contexts are direct formal analogues of one another within the diffusion theory, although their relationship to the many-body problem is very different.

In the continuum Green's-function approach,⁶ the fact that the kinetic energy for an M -particle system is of the form

$$T = \sum_{i=1}^M \nabla_i^2, \quad (2)$$

allows the Schrödinger equation in imaginary time τ to be viewed as a diffusion equation. The propagator for the diffusion equation is simulated by a continuous random walk in the configuration space of the particles (a $3M$ -dimensional space). The potential V (which must be diagonal in the coordinate-space representation and includes external potential *and* interaction terms) gives rise to "branching" of walkers (i.e., producing copies of them-

selves) at a rate proportional to $-V$. In practice, an important aspect of the Green's-function Monte Carlo approach is the use of a guiding (or trial) function which gives much better statistical estimators of physical quantities. While this modification introduces a drift term into the equation, it does not alter the basic idea of realizing the imaginary-time Schrödinger equation as a diffusion process with branching.

Green's-function Monte Carlo methods have also been applied more recently to lattice problems.¹²⁻¹⁴ However, in these cases, the imaginary-time propagation does not reduce to a continuous diffusion process, although (for appropriate Hamiltonians) the Green's function is positive and can be simulated by a random walk with branching in the (discrete) configuration space of the particles. In the rest of this paper we will not consider these discrete-space versions and, in further discussion of the Green's-function Monte Carlo approach, we will mean specifically the original continuum version for the imaginary-time Schrödinger equation.

The auxiliary-field approach is very different in spirit from the Green's-function method. Here we make explicit use of the fact that the interacting Hamiltonian is a sum of one- and two-body terms. The form of the one-body terms is not important; in particular, no use is made of any special form of the kinetic energy or external potential. The two-body terms are assumed to be a sum of squares of one-body operators. These two-body interaction terms are replaced, using the Hubbard-Stratonovitch transformation,^{15,16} with Gaussian random auxiliary fields \mathbf{x} which act as time-dependent external potentials on the particles

$$\exp(-\beta H) = \int dG[\mathbf{x}] U_{\mathbf{x}}(\beta, 0), \quad (3)$$

where $U_{\mathbf{x}}(\beta, 0)$ is the propagator over the imaginary-time interval $[0, \beta]$ for an independent-particle Hamiltonian which includes the action of the auxiliary fields \mathbf{x} on the particles and $\int dG[\mathbf{x}]$ which gives a Gaussian distribution of \mathbf{x} . (These fields can be considered as mediating fields for the two-body interaction in somewhat the same way as the phonon fields mediate the electromagnetic interaction in electrodynamics.) In this way, the interacting problem is replaced by an integral over an ensemble of noninteracting systems in a set of random τ -varying external fields. We will discuss in detail below how this is achieved. It is worth pointing out at this stage that the Hubbard-Stratonovitch transformation for a particular many-body problem is not unique^{11,16} and that different choices may have very different numerical behavior.

The auxiliary-field approach has been used for some time in calculating finite-temperature properties for the grand canonical ensemble.¹⁷ Here the basic quantity to be calculated is the grand sum for the many-body Hamiltonian at a given inverse temperature β , i.e., the trace of the propagator $\exp[-\beta(H - \mu N)]$ over a complete set of fermion states. Again, the many-body propagator is expressed in the form given in Eq. (3) as an integral of independent-particle propagators and the grand sum is the integral of the traces of these propagators. The point of crucial importance¹⁷ to the utility of this approach is that the trace over all fermion states of each propagator

$U_{\mathbf{x}}(\beta, 0)$ can be written very compactly as the determinant of the operator $I + U_{\mathbf{x}}(\beta, 0)$ considered as a matrix on the space of single-particle wave functions. This "tracing out of the fermion variables" hides the fact that each member of a complete set of Slater-determinant trial states is being propagated in a manner exactly paralleling the projection method, where only one fermion state $|\Psi_t\rangle$ is propagated.¹⁸ Our principal results can, in fact, be applied almost without modification to the grand canonical formulation at large β .

A. Representation of states

For the purposes of this work, we wish to concentrate on the way in which the propagated many-body state in Eq. (1) is represented as a result of the representation of the propagator given in Eq. (3). We will assume that the initial state is an antisymmetrized product of single-particle orbitals; in other words, a single Slater determinant. (In the practical implementation of the auxiliary-field projection approach, this assumption is essential.⁷⁻⁹) The important observation now is that a single Slater determinant propagated by any independent-particle Hamiltonian always remains as a single Slater determinant,^{7,18} each single-particle orbital in the antisymmetrized product just propagates independently. The propagated many-body state in Eq. (1) is then automatically represented as an integral of Slater determinants, one for each choice of auxiliary fields

$$|\Phi(\beta)\rangle = \int dG[\mathbf{x}] |\Psi_{\mathbf{x}}\rangle, \quad (4)$$

where $|\Psi_{\mathbf{x}}\rangle$ is the Slater determinant propagated in fields \mathbf{x} :

$$|\Psi_{\mathbf{x}}\rangle \equiv U_{\mathbf{x}}(\beta, 0) |\Psi_t\rangle. \quad (5)$$

The distribution of auxiliary fields thus gives rise to a distribution of Slater determinants. This distribution of Slater determinants in turn gives rise to a distribution of matrix elements $\langle \Psi_t | O | \Psi_{\mathbf{x}} \rangle$ in the course of evaluating the physical expectation value of an operator O .⁷

The central question addressed in the present work is the following: "How does this distribution of determinants evolve with imaginary time?" The answer, which we derive below, is that it obeys a diffusionlike equation. This emerges when we change the coordinates labeling the propagated Slater determinants from the auxiliary-field variables \mathbf{x} to appropriately chosen intrinsic coordinates Ψ for the normalized Slater determinants themselves. Then the propagated state is written as an integral over these intrinsic coordinates, rather than over the auxiliary fields

$$|\Phi(\beta)\rangle = \int f(\Psi; \beta) |\Psi\rangle d\Psi. \quad (6)$$

(We incorporate the norm of $|\Psi_{\mathbf{x}}\rangle$ into the weight function f and $|\Psi\rangle$ is normalized.) The object of study then becomes the weight or distribution function $f(\Psi; \beta)$, rather than the auxiliary fields themselves. However, we note that, although we have hidden the fields in the notation of Eq. (6), their coupling to the particles still determines the evolution of the function f . At $\beta=0$, the dis-

tribution is a δ function at the trial state Ψ_t . We will find that, although the evolution of the many-body state $|\Phi(\beta)\rangle$ depends only on the original many-body Hamiltonian, the evolution of the weight function f depends on the particular choice of Hubbard-Stratonovitch transformation and that f is different for different choices. This is not too surprising when we realize that the basis functions (viz., all Slater determinants) used to represent Φ in Eq. (6) form a vastly overcomplete set.

The representation of the ground state is governed by the asymptotic behavior of $f(\Psi;\beta)$ is $\beta \rightarrow \infty$. The natural question of what determinants predominate in the representation of Φ translates into the question of where f is peaked. Perhaps not surprisingly, we find that f is often strongly concentrated near the classical mean-field solutions.

Conventional discussions of auxiliary-field methods focus on a matrix element⁷⁻⁹ or trace¹⁷ as a scalar functional of the fields. The essential viewpoint (admittedly an unconventional one) advocated in the present work is from "inside" such a matrix element. From this perspective, we see the Hubbard-Stratonovitch transformation as a formal mapping of the original many-body problem onto a stochastic dynamical process on the set of Slater determinants. The intuitive picture behind the derivation of a diffusionlike equation of motion for $f(\Psi;\tau)$ is as follows. Given an initial Slater determinant Ψ_t , a particular choice of auxiliary fields induces (via the corresponding Hubbard-Stratonovitch propagator) a "walk" of Ψ through the set of Slater determinants. (It also changes the normalization of Ψ , giving rise to "branching" terms.) The Gaussian random selection of auxiliary fields will then give rise to a random walk of Ψ through the set of Slater determinants. It is a familiar fact that, in general, random-walk behavior of a set of particles gives rise to a diffusion equation for their density.¹⁹ In this case, the "particles" are the points Ψ and the density is the function $f(\Psi;\tau)$.

B. Measurement and the sign problem

In the practical implementation of the auxiliary-field projection method, quantities are calculated by evaluating the overlap of the projected state $|\Phi(\beta)\rangle$ with the initial trial state $|\Psi_t\rangle$. For example, for sufficiently large β , the ground-state energy ϵ_0 is calculated⁷ as

$$\epsilon_0 = \frac{\langle \Psi_t | H | \Phi(\beta) \rangle}{\langle \Psi_t | \Phi(\beta) \rangle} = \frac{\int dG[\mathbf{x}] \langle \Psi_t | H | \Psi_x \rangle}{\int dG[\mathbf{x}] \langle \Psi_t | \Psi_x \rangle}. \quad (7)$$

Unfortunately, although $\langle \Psi_t | \Phi(\beta) \rangle$ must be positive, because the fields \mathbf{x} are time dependent, the matrix elements $\langle \Psi_t | \Psi_x \rangle$ are not always positive. Except in special circumstances, the average sign

$$\sigma(\beta) = \frac{\int dG[\mathbf{x}] \langle \Psi_t | \Psi_x \rangle}{\int dG[\mathbf{x}] |\langle \Psi_t | \Psi_x \rangle|} \quad (8)$$

of these matrix elements has been found to become very small for large β , leading to the ill-conditioned statistical estimators which constitute the "minus-sign problem."

In the grand canonical approach, determinants of the operator $I + U_x(\beta,0)$ replace these matrix elements in expressions analogous to Eqs. (7) and (8), and share their lack of positivity as functionals of $\mathbf{x}(\tau)$. Comparable rates of decay of $\sigma(\beta)$ have been found for both grand canonical and projection approaches in numerical studies.^{10,18} We emphasize that the sign problem is a consequence of the representation leading to Eq. (7), not of the original many-body problem in Eq. (1).

Using the equivalent form of the propagated state given in Eq. (6), the average sign in the auxiliary-field projection method can be reexpressed as an average over our distribution f :

$$\sigma(\beta) = \frac{\int f(\Psi;\beta) \langle \Psi_t | \Psi \rangle d\Psi}{\int f(\Psi;\beta) |\langle \Psi_t | \Psi \rangle| d\Psi}. \quad (9)$$

The integrals in the numerator and denominator of Eq. (9) couple to different symmetries of the function f ; the numerator projects out the "odd" component of f and the denominator the "even" component (we will define later precisely what "odd" and "even" mean). We will see that the odd components of f always decay exponentially with β at a rate greater than that for the even components. The difference between these two rates equals the rate of exponential decay of the sign $\sigma(\beta)$ for large β . (For exceptional problems with special symmetries, such as the half-filled Hubbard model with a spin-coupled auxiliary field, the odd and even components may decay at the same rate and the rate of decay of the sign is zero.)

The auxiliary-field projection approach for interacting fermion systems attracted considerable attention recently when an intriguing suggestion was made^{8,9} by Sorella *et al.*, in the application of the method to the two-dimensional Hubbard model. They proposed that the sign problem that occurs in this method can be circumvented with negligible (or in certain cases, zero) error in the calculated physical quantities. This is achieved by replacing by their absolute value the matrix elements which occur in Eq. (7) in summing over auxiliary fields. The variance of statistical estimators in the method is thereby greatly reduced. Surprisingly, this counter-intuitive suggestion has yielded remarkably accurate results in certain cases. Although the initial promise of this approach has not been entirely borne out in all cases, and its results are not uniformly satisfactory,^{18,20} a better understanding of the successes of the approximation in terms of the Hamiltonian of the system and the Hubbard-Stratonovitch transformation used is clearly an important goal, as is the identification of situations where it is likely to fail.

A word about minus-sign problems in the continuum Green's-function Monte Carlo method for fermions: In the Green's-function approach,^{3,21} the minus signs occur essentially because the lowest-energy solution of the diffusion equation on the space of configurations of the system is nodeless. This solution is the boson ground state. However, in solving fermion problems, we wish to confine our attention to antisymmetric wave functions only. In the "release-node" approach, minus signs occur when walkers cross the nodes of a reference antisymmetric guiding wave function.³ The number of minus

signs and the number of plus signs (i.e., the number of “positive walkers” and “negative walkers”) increase exponentially compared to the difference between them, which is the number we need to calculate. The rate of this exponential increase equals the difference between the boson and fermion ground-state energies,³ or alternatively, the difference between the energy of the nodeless solution of the diffusion equation and that of the lowest antisymmetric solution.

Although it is well known¹¹ that fermion Monte Carlo simulations of both the auxiliary-field and Green’s-function type generally have problems with “minus signs,” it has not been clear if a precise relationship exists between the minus signs which occur in the two approaches. In either case, the existence of terms with negative sign gives rise to very poor statistics in the quantities we wish to evaluate. Of course, a “sign problem” is built into any representation of a real wave function by a linear combination of preordained functions. For a given state, the latter can always be chosen once the state is known so that their coefficients are non-negative. The problem is that of deciding beforehand. In particular, if the coefficients are regarded as a probability distribution on the index space, attention to this point becomes mandatory. Both Green’s-function Monte Carlo and auxiliary-field projection Monte Carlo exacerbate this problem by starting with an overcomplete basis—all of configuration space rather than $1/N!$ of it in the Green’s-function approach, and all Slater determinants rather than a finite set of them in the auxiliary-field approach. However, none of these observation tells us whether the average sign will be finite, algebraically small, or exponentially small in the limit of large imaginary-time propagation.

We will show in this paper that there is a very close mathematical connection between the behavior of the two approaches which can be understood in terms of a general property of diffusion equations, viz., that their lowest-energy solutions are nodeless. The connection between the diffusion and the original many-body problem is very different in each case, as is the space in which the diffusion process takes place. In the case of the Green’s-function approach, the diffusion occurs in the configuration space of the particles and arises because of the ∇^2 form of the kinetic energy in the Schrödinger equation. In the auxiliary-field approach, the diffusion occurs in the set of M -particle normalized Slater determinants and arises because Gaussian fluctuations of the auxiliary fields induce a random walk on the set of Slater determinants. The nodeless solution has a direct physical interpretation³ (viz., the boson ground state) in the Green’s-function approach but does not, to our knowledge, have any such interpretation in the auxiliary-field approach. In either case, the average sign decays exponentially, but the rate of decay is governed by very different factors in the two approaches.

Incidentally, we note that the noninteracting problem (i.e., no two-body terms) has a very special status within the auxiliary-field approach; it is the case for which the coupling of the auxiliary fields to the particles vanishes and the Hubbard-Stratonovitch ensemble of noninteract-

ing systems reduces to a single system, viz., the *real* noninteracting system, and there is no longer any stochastic aspect to the approach. This is quite different from the status of the noninteracting problem in the Green’s-function Monte Carlo approach; there the random walk of the particles continues to be effective but now each particle walks independently of the others. From the point of view of implementation as a stochastic process, the analogue of the noninteracting limit in the auxiliary-field approach is the infinite-mass limit in Green’s-function Monte Carlo.

The rest of this paper is organized as follows. In Sec. II, we study the auxiliary-field projection in the specific case of the two-site Hubbard model. This serves both to introduce some notation and also to give a graphical picture of propagation in the set of normalized Slater determinants. Turning to the properties of the auxiliary-field approach in a general context, some relevant geometrical properties of the set of normalized Slater determinants as a manifold are discussed in Sec. III, and in Sec. IV a diffusionlike equation is derived for the propagation of states in the auxiliary fields. We discuss some consequences of this diffusion picture in Sec. V and outline the general conclusions of this study in Sec. VI. The form of some coefficients in the diffusion equation are derived in the Appendix.

II. EXAMPLE: THE TWO-SITE HUBBARD MODEL

Let us take as a simple example the case of the Hubbard model²² of a paramagnetic hydrogen molecule; i.e., the Hubbard model with two sites and two electrons with opposite spin. We take this example because the relevant set of Slater determinants can easily be visualized, and yet it displays a nontrivial behavior in the evolution of the states. This will serve to introduce both the auxiliary-field method and the geometry of the set of normalized Slater determinants in a specific case, and also to focus on some of the features of the problem which will be treated in a more abstract general setting subsequently. The Hamiltonian of the system²² is

$$H = -t \sum_{\sigma=\uparrow,\downarrow} (c_{1\sigma}^\dagger c_{2\sigma} + c_{2\sigma}^\dagger c_{1\sigma}) + U \sum_{i=1,2} n_{i\uparrow} n_{i\downarrow}, \quad (10)$$

where σ and i are spin and site indices, c^\dagger and n are the creation and number operators, and t and U are the hopping and on-site interaction terms, respectively. We will assume a repulsive on-site interaction so that $U > 0$. In the auxiliary-field approach, we express the interaction term $n_{i\uparrow} n_{i\downarrow}$ as a square of one-body terms plus some additional one-body terms:^{23,24}

$$n_{\uparrow} n_{\downarrow} = -\frac{1}{2}(n_{\uparrow} - n_{\downarrow})^2 + \frac{1}{2}(n_{\uparrow} + n_{\downarrow}). \quad (11)$$

For the rest of the discussion, we will neglect the term $\frac{1}{2}(n_{\uparrow} + n_{\downarrow})$ since it involves only a trivial shift in the chemical potential and does not affect any of the dynamics we are interested in. Thus, we rewrite the Hamiltonian as

$$H = -t \sum_{\sigma=\uparrow,\downarrow} (c_{1\sigma}^\dagger c_{2\sigma} + c_{2\sigma}^\dagger c_{1\sigma}) - \frac{1}{2}U \sum_{i=1,2} (n_{i\uparrow} - n_{i\downarrow})^2. \quad (12)$$

For convenience, we define the quantities

$$H_0 = -t \sum_{\sigma=\uparrow,\downarrow} (c_{1\sigma}^\dagger c_{2\sigma} + c_{2\sigma}^\dagger c_{1\sigma}), \quad (13)$$

which includes all one-body terms in H , and

$$H_i = \sqrt{U} (n_{i\uparrow} - n_{i\downarrow}) \quad (14)$$

for $i=1,2$, whose squares give the two-body interactions in H .

We now expand the propagator generated by this Hamiltonian according to standard auxiliary-field approach. The many-body propagator $\exp(-\tau H)$ can be written trivially as a product of propagators over short "time slices," each of length $\Delta\tau$. On each time slice propagator by the product of the propagators for the individual terms in the Hamiltonian:

$$\exp(-\Delta\tau H) = \exp(-\Delta\tau H_0) \prod_{i=1,2} \exp\left[\frac{\Delta\tau}{2}(H_i)^2\right] + O(\Delta\tau^2). \quad (15)$$

Thus, we obtain the Trotter²⁵ expansion

$$\begin{aligned} \exp(-\tau H) &= \lim_{m \rightarrow \infty} \prod_{l=1}^m \exp(-\Delta\tau H) \\ &= \lim_{m \rightarrow \infty} \prod_{l=1}^m \left[\exp(-\Delta\tau H_0) \right. \\ &\quad \left. \times \prod_{i=1}^2 \exp\left[\frac{1}{2}\Delta\tau(H_i)^2\right] \right], \quad (16) \end{aligned}$$

where $\Delta\tau \equiv \tau/m$. In the Hubbard-Stratonovitch transformation,^{15,16} the two-body propagators are replaced by an integral over auxiliary fields (which can be considered to mediate the two-body interaction) by means of the following operator identity:

$$\exp\left[\frac{1}{2}\Delta\tau(H_i)^2\right] = \int_{-\infty}^{+\infty} \exp(-xH_i) \frac{e^{-x^2/(2\Delta\tau)}}{\sqrt{2\pi\Delta\tau}} dx. \quad (17)$$

We may now express our original many-body propagator as the infinite time-slice limit of the integral over Gaussian auxiliary fields $\{x_{il}\} = \mathbf{x}$,

$$\begin{aligned} \exp(-\tau H) &= \lim_{m \rightarrow \infty} \prod_{l=1}^m \exp(-\Delta\tau H_0) \\ &\quad \times \prod_{i=1}^2 \int_{-\infty}^{+\infty} \exp(-x_{il}H_i) \\ &\quad \times \frac{e^{-x_{il}^2/(2\Delta\tau)}}{\sqrt{2\pi\Delta\tau}} dx_{il}, \\ &= \lim_{m \rightarrow \infty} \int dG[\mathbf{x}] U_{\mathbf{x}}(\tau, 0), \quad (18) \end{aligned}$$

where

$$U_{\mathbf{x}}(\tau, 0) = \prod_{l=1}^m \left[\exp(-\Delta\tau H_0) \prod_{i=1}^2 \exp(-x_{il}H_i) \right] \quad (19)$$

is the Hubbard-Stratonovitch propagator for a particular choice $\{x_{il}\}$ of auxiliary fields which couple to the electrons during the l th time slice through the operators H_i ,

and

$$dG[\mathbf{x}] = \prod_{i=1}^m \prod_{l=1}^2 \frac{e^{-x_{il}^2/(2\Delta\tau)}}{\sqrt{2\pi\Delta\tau}} dx_{il} \quad (20)$$

is the Gaussian measure of the x fields on m time slices.

Note^{7,18} that each Hubbard-Stratonovitch propagator acts on a Slater determinant of M states

$$|\Psi\rangle = |\underline{u}_1, \dots, \underline{u}_M\rangle = (M!)^{-1/2} \prod_{i=1}^M c_i^\dagger * \underline{u}_i |0\rangle \quad (21)$$

to give another Slater determinant $|\Psi'\rangle = |\underline{u}'_1, \dots, \underline{u}'_M\rangle$, where we have used the general matrix notation for many-body operators over an N -dimensional single-particle space

$$c_i^\dagger * \underline{u} = \sum_{j=1}^N c_j^\dagger u_j. \quad (22)$$

The action of $U_{\mathbf{x}}(\tau, 0)$ as a many-body operator is simply to propagate each individual state \underline{u} in the Slater determinant with the one-body operator $\underline{U}_{\mathbf{x}}(\tau, 0)$:

$$\underline{u}'_j = \underline{U}_{\mathbf{x}}(\tau, 0) * \underline{u}_j. \quad (23)$$

In this sense, the Hubbard-Stratonovitch transformation replaces the interacting system with a noninteracting system in a random time-varying field.

In practice, some finite number m of time slices is used to approximate the infinite- m limit. Also,⁷⁻⁹ long-time propagation of the states \underline{u}_i in the Slater determinant tends to produce linear dependence in the propagated wave functions \underline{u}'_i . This corresponds to a collapse into the boson ground state. As was first suggested in Ref. 7, this numerical instability can be simply avoided by frequent reorthogonalization of the states \underline{u}'_i as they propagate. This orthogonalization does not change the Slater determinant represented by \underline{u}'_i and we will not refer to it further.

Turning now to the set of normalized Slater determinants, we consider specifically the paramagnetic, half-filled two-site problem. We have two electrons, one with spin up and the other with spin down. The spin-up state \underline{u}_\uparrow is a linear combination of the two-site orbitals:

$$\underline{u}_\uparrow = \cos\theta_1 |1\uparrow\rangle + \sin\theta_1 |2\uparrow\rangle. \quad (24)$$

Similarly, the spin-down state can be written as

$$\underline{u}_\downarrow = \cos\theta_2 |1\downarrow\rangle + \sin\theta_2 |2\downarrow\rangle. \quad (25)$$

Thus, the pair of angles (θ_1, θ_2) uniquely specifies a two-particle, paramagnetic Slater determinant $|\underline{u}_\uparrow, \underline{u}_\downarrow\rangle$ for the two-site problem. Since the Hubbard-Stratonovitch Hamiltonian we are using has no spin-flip terms in it, a Slater determinant which starts with one state pure spin up and another state pure spin down will remain so throughout its evolution. Thus, we need only consider the set of states described by the parameters (θ_1, θ_2) . Clearly, the following periodicities hold:

$$|\Psi(\theta_1 \pm \pi, \theta_2)\rangle = -|\Psi(\theta_1, \theta_2)\rangle, \quad (26a)$$

$$|\Psi(\theta_1, \theta_2 \pm \pi)\rangle = -|\Psi(\theta_1, \theta_2)\rangle, \quad (26b)$$

$$|\Psi(\theta_1 \pm \pi, \theta_2 \pm \pi)\rangle = |\Psi(\theta_1, \theta_2)\rangle. \quad (26c)$$

We can restrict the values of (θ_1, θ_2) to the fundamental diamond-shaped region **D** with the vertices $(0, \pi)$, $(\pi, 0)$, $(0, -\pi)$, and $(-\pi, 0)$, as shown in Fig. 1, identifying opposite edges in accordance with Eq. (26c). It is important that we always consider Ψ and $-\Psi$ as separate points on the set of normalized Slater determinants. Indeed, this distinction will be crucial to the appearance of the minus-sign problem in auxiliary-field fermion simulations. (In general, we will denote the state $|\Psi\rangle$ in the usual ket notation when we are considering it as a state in the Hilbert space and as Ψ when we are considering it as a point on the manifold of normalized Slater determinants.)

The point $(0,0)$ represents the state where both particles are on site 1, and at $(\pi/2, \pi/2)$ both particles are on site 2, as denoted by the symbols in Fig. 1. The points $(\pi/2, 0)$ and $(0, \pi/2)$ represent the ground states in the infinite- U limit, where the particles are on opposite sites. The ground state of the noninteracting system ($U=0$) is the point $(\pi/4, \pi/4)$, where both the spin-up and spin-down particles are in the symmetric combination of the two sites $(|1\rangle + |2\rangle)/\sqrt{2}$. Inversion of the parameter space about the point $(\pi/4, \pi/4)$ (i.e., the transformation $\theta_1 \rightarrow \pi/2 - \theta_1$, $\theta_2 \rightarrow \pi/2 - \theta_2$) is equivalent to swapping sites 1 and 2. Reflection in the line $\theta_1 = \theta_2$ is equivalent to swapping spin-up and spin-down. The states along the line $\theta_2 = \pi/2 - \theta_1$ (the dashed line in Fig. 1) have particle-hole symmetry^{26,27} of the kind usually referred to in connection with the half-filled Hubbard model, which, in this two-site case, amounts to invariance under the combined action of swapping spins and sites.

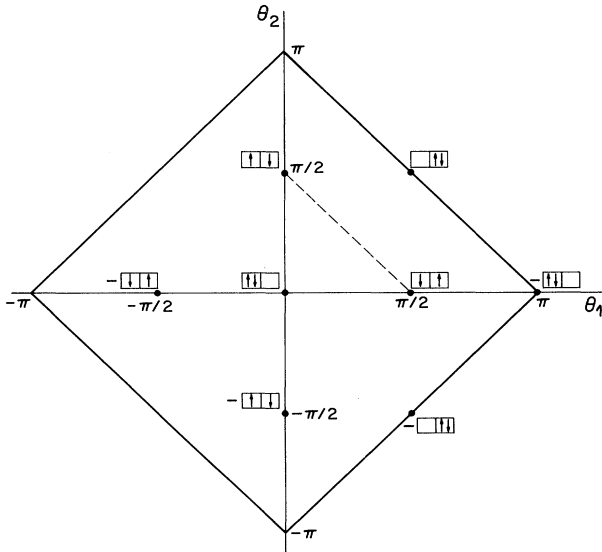


FIG. 1. The manifold of Slater determinants considered in the two-site Hubbard model with two electrons of opposite spin. The angles θ_1 and θ_2 are defined in Eqs. (24) and (25). The symbols at particular points represent the states corresponding to those points, as discussed in the text. Only the region $0 \leq \theta_1 \leq \pi/2$, $0 \leq \theta_2 \leq \pi/2$ is shown in Figs. 2 and 3. The dashed line denotes the set of states with particle-hole symmetry in that region.

The evolution of an initial trial state $\Psi_t = \Psi(\theta_{1,t}, \theta_{2,t})$ in a particular choice of auxiliary fields can then be viewed as a trajectory in the two-dimensional parameter space, and the distribution of Slater determinants obtained from the propagation of the initial state for a time τ in the Gaussian distribution (Eq. 20) of auxiliary fields $\{x_{il}\}$ gives a distribution $f(\theta_1, \theta_2; \tau)$ of the parameters. The many-body state

$$|\Phi(\tau)\rangle = \exp(-\tau H)|\Psi_t\rangle$$

is given by the integral

$$|\Phi(\tau)\rangle = \int_{\mathbf{D}} f(\theta_1, \theta_2; \tau) |\Psi(\theta_1, \theta_2)\rangle d\theta_1 d\theta_2. \quad (27)$$

In this notation, the initial distribution is a δ function:

$$f(\theta_1, \theta_2; 0) = \delta(\theta_1 - \theta_{1,t}) \delta(\theta_2 - \theta_{2,t}), \quad (28)$$

Shown in Fig. 2 is a sampling²⁸ of the distribution f for

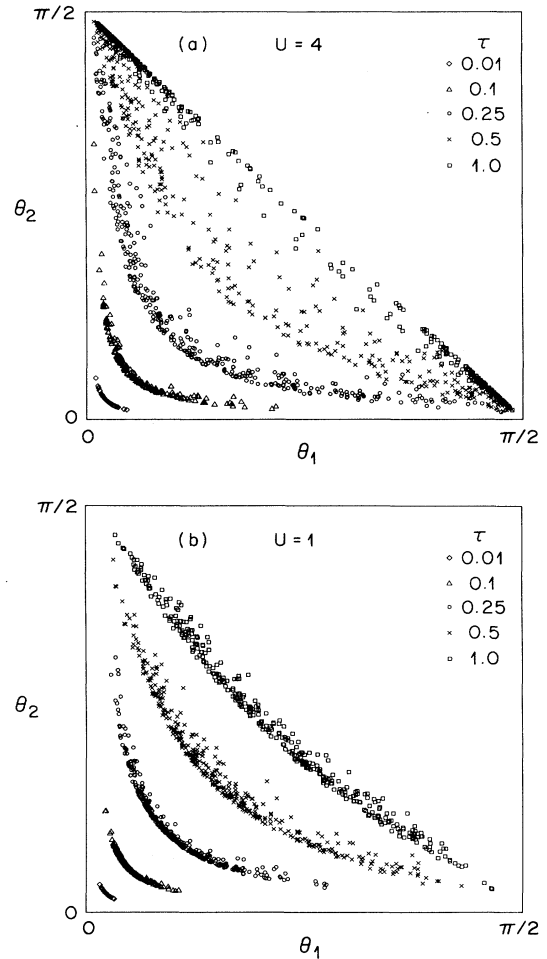


FIG. 2. Propagation of states for the usual two-site Hubbard model in the random auxiliary fields as a function of imaginary time τ for values of $\tau=0.01, 0.1, 0.25, 0.5$, and 1.0 . The hopping coefficient $t=1$. The on-site repulsion $U=4$ in (a), and $U=1$ in (b). A representative set of points from the distribution at each value of τ . The change in the overall normalization of the distribution with τ is not represented here.

various values of τ , starting from the point $\Psi(0,0)$ at $\tau=0$. In Fig. 2(a), the on-site repulsion $U=4$, and in Fig. 2(b), $U=1$. In the absence of interaction terms (i.e., for $U=0$), the initial point would not spread out into a distribution, but rather drift as a single point along the line $\theta_1=\theta_2$, eventually converging exponentially to the point $(\pi/4, \pi/4)$, the ground state of the noninteracting system. Interaction-induced diffusion spreads the initial point around a set of hyperbolic “fronts” which advance, driven by the drift term, towards the line $\theta_2=\pi/2-\theta_1$. A greater concentration of points towards the ends of the line for $U=4$ is indicative of stronger Heitler-London-like correlations.

The collapse of the distribution onto the diagonal line for all values of the interaction parameter U is a consequence of the particle-hole symmetry of the half-filled Hubbard model.²⁷ In general, such a collapse will be indicative of a conservation law obeyed by all the Hubbard-Stratonovitch fields and the noninteracting Hamiltonian and is not generic for all systems. This is demonstrated in Fig. 3, which shows the asymptotic distribution $f(\Psi;\beta)$ as $\beta\rightarrow\infty$ when the particle-hole symmetry in the noninteracting Hamiltonian is altered by the addition of a potential of -1 to site 1, destroying the equivalence of the two sites. The distribution no longer collapses onto a line as $\beta\rightarrow\infty$.

This two-site example has served to introduce the concept of the auxiliary-field projection method as a dynamical process on the manifold of normalized Slater determinants. In the rest of this paper we will examine the evolution of the representation of many-body states in the auxiliary-field projection method in the general case. Because of the high dimensionality of the manifold of Slater determinants, it is not, in general, easy to visualize the evolution of the representation, as it has been possible in

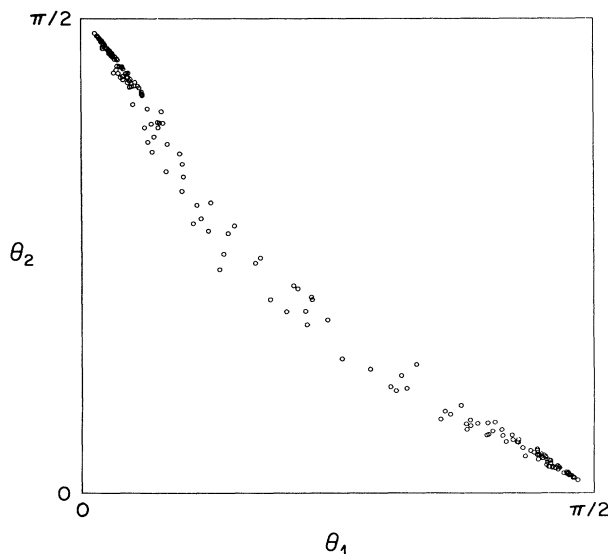


FIG. 3. The asymptotic distribution of states (this sample for $\tau=2$) for the two-site Hubbard model with an asymmetric potential on the sites. A potential of -1 is added on site 1. The hopping coefficient $t=1$ and the on-site repulsion $U=4$.

the above example. However, the simple example given here exhibits many characteristics of the general situation without being itself unduly abstract.

III. THE MANIFOLD OF SLATER DETERMINANTS

Since we want to study the evolution of the distribution of Slater determinants which arise in the auxiliary-field approach in an intrinsic way, as we did in the two-site example in Sec. II, we want to have some way of parametrizing the set of normalized Slater determinants in the general case. If we expect to be able to describe the evolution of the weight function f by a differential equation of some type, then we need to be able to differentiate and integrate with respect to the parameters. In mathematical language, we want to view the set of normalized Slater determinants as a differential manifold. For our immediate purposes, this will amount to nothing more than setting up local coordinates about each point.

We assume that there are N available single-particle states so that the M -particle fermion space has dimension ${}^N C_M$. A point (state) $|\Psi\rangle$ in the M -particle Hilbert space belongs to the set \mathbf{D} of normalized Slater determinants if it is the antisymmetrized product of some set of M orthonormal one-particle functions \underline{u}_i , $i=1, M$:

$$|\Psi\rangle = [M!]^{-1/2} \prod_{i=1}^M c^\dagger * \underline{u}_i |0\rangle. \quad (29)$$

Note that \mathbf{D} is *not* a linear subspace of the Hilbert space; the sum of two Slater determinants is not necessarily a Slater determinant.

To define a local coordinate system about the point Ψ , consider the number of independent infinitesimal changes we can make to the set of vectors \underline{u}_i in Eq. (29) to generate different Slater determinants: Suppose we extend this set of M orthonormal vectors to a full orthonormal basis \underline{u}_i , $i=1, N$, for the single-particle Hilbert space. The first M vectors are the states occupied in the Slater determinant and the last $(N-M)$ states are unoccupied. To each \underline{u}_i , $i=1, M$, we can add an amount ε_{ij} of the vector \underline{u}_j , $j=1, N$. However, the addition of any state \underline{u}_j for $j \leq M$ does not change the Slater determinant (it only changes its normalization), and so the independent parameters which specify distinct nearby Slater determinants are ε_{ij} , with $1 \leq i \leq M$ and $M+1 \leq j \leq N$. Thus, we need $M(N-M)$ coordinates ε_{ij} to specify all normalized Slater determinants in the infinitesimal region near $|\Psi\rangle = |\underline{u}_1, \dots, \underline{u}_M\rangle$. Thus, the dimension of the manifold \mathbf{D} is $M(N-M)$.

As an example, in the two-site Hubbard model, the single-particle Hilbert space has dimension 4, arising from two site and two spin indices. The full manifold of two-particle normalized Slater determinants then has dimension $2(4-2)=4$. However, we used the conservation of spin by the Hubbard-Stratonovitch propagators to restrict our attention in Sec. II to the two-dimensional $S_2=0$ submanifold. As it turned out, in the half-filled model with particle-hole symmetry, we could have further limited the dynamics to the one-dimensional manifold $\theta_1=\pi/2-\theta_2$ of states with this symmetry.

The vectors pointing along the local coordinate axes

$$\hat{\epsilon}_{ij} \equiv (\underline{c}^\dagger * \underline{u}_j)(\underline{u}_i * \underline{c})|\Psi\rangle \quad (30)$$

for $i=1, M$ and $j=M+1, N$, give us a basis for the vector space of all tangents to the manifold at the point Ψ defined in Eq. (29). Each of these basis vectors is a Slater determinant in which the state \underline{u}_j replaces the state \underline{u}_i in $|\Psi\rangle$. This corresponds to a particle-hole excitation on $|\Psi\rangle$, where the particle state is \underline{u}_j and the hole is \underline{u}_i .

The distance $d\underline{l}$ between two points on \mathbf{D} infinitesimally close together, $|\Psi\rangle = |\underline{u}_1, \dots, \underline{u}_M\rangle$ and $|\Psi'\rangle = |\underline{u}'_1, \dots, \underline{u}'_M\rangle$, where

$$\underline{u}'_i = \underline{u}_i + \sum_{j=M+1}^N \epsilon_{ij} \underline{u}_j, \quad (31)$$

is defined in the obvious way from the lengths of vectors in the many-body Hilbert space as

$$(d\underline{l})^2 = \|\Psi\rangle - |\Psi'\rangle\|^2 = \sum_{i=1}^M \sum_{j=M+1}^N (\epsilon_{ij})^2. \quad (32)$$

The distance defined in this way is independent of the particular local orthonormal coordinate system used. Similarly, the inner product between the tangents to two curves $\Psi(t)$ and $\Psi'(t)$ passing through a common point is given by

$$\begin{aligned} \frac{d\Psi(t)}{dt} \cdot \frac{d\Psi'(t)}{dt} &= \left\langle \frac{d\Psi(t)}{dt} \left| \frac{d\Psi'(t)}{dt} \right. \right\rangle \\ &= \sum_{i=1}^M \sum_{j=M+1}^N \frac{d\epsilon_{ij}}{dt} \frac{d\epsilon'_{ij}}{dt}. \end{aligned} \quad (33)$$

Again, this definition of inner product is independent of the orthonormal coordinate system used in the summation.

The gradient of a function $f(\Psi)$ defined on \mathbf{D} can be written as

$$\nabla_{\Psi} f = \sum_{l=1}^M \sum_{m=M+1}^N \hat{\epsilon}_{lm} \frac{\partial f}{\partial \epsilon_{lm}}. \quad (34)$$

The gradient of any function f defines a vector field on \mathbf{D} . For any curve $\Psi(t)$ on \mathbf{D} , the derivative of f along the curve is given by

$$\frac{df}{dt} = \frac{d\Psi(t)}{dt} \cdot \nabla_{\Psi} f. \quad (35)$$

Finally, the local orthonormal coordinates can be used to define a measure or area function $d\Psi$ on the manifold in a natural way. The area of an infinitesimal region near a point Ψ , specified in local orthonormal coordinates by $0 < \epsilon_{ij} < \Delta\epsilon_{ij}$, is

$$\Delta\Psi = \prod_{i=1}^M \prod_{j=M+1}^N \Delta\epsilon_{ij}. \quad (36)$$

(This is a straightforward generalization of the usual idea of a surface area for a two-dimensional manifold). The integral of a function $f(\Psi)$ defined on the manifold \mathbf{D} with respect to this measure is denoted by $\int_{\mathbf{D}} f(\Psi) d\Psi$.

IV. DIFFUSIVE BEHAVIOR OF STATES

With these standard geometrical concepts defined for the particular case of the manifold of Slater determinants, we proceed to consider the action of the Hubbard-Stratonovitch Hamiltonian on a many-body wave function represented as an integral of Slater determinants:

$$|\Phi\rangle = \int_{\mathbf{D}} f(\Psi) |\Psi\rangle d\Psi. \quad (37)$$

To each function f on \mathbf{D} there corresponds a many-body wave function $|\Phi\rangle$, as defined in Eq. (37). For example, the points shown in Fig. 2 represent a sampling of the function f for various values of τ in the case of the two-site Hubbard model when the initial f is a δ function at $(\theta_1, \theta_2) = (0, 0)$. Every many-body wave function can be represented in this way, but the representation is not unique, since the set of all Slater determinants is over-complete as a basis for the Hilbert space. Given a particular representation of the initial many-body state,

$$|\Phi(0)\rangle = \int_{\mathbf{D}} f(\Psi; 0) |\Psi\rangle d\Psi, \quad (38)$$

we will represent the state $|\Phi(t)\rangle$ which follows the imaginary-time evolution of the many-body Hamiltonian according to the equation of motion

$$\frac{d}{d\tau} |\Phi(\tau)\rangle = -H |\Phi(\tau)\rangle, \quad (39)$$

in a similar form

$$|\Phi(\tau)\rangle = \int_{\mathbf{D}} f(\Psi; \tau) |\Psi\rangle d\Psi. \quad (40)$$

Just as the function $f(\Psi; 0)$ used to represent the initial state is not unique, the evolution of $|\Phi(\tau)\rangle$ does not uniquely determine the evolution of $f(\Psi; \tau)$. Specifically, will derive the equation of motion for $f(\Psi; \tau)$ which arises naturally from the Hubbard-Stratonovitch representation of the many-body propagator given in Eq. (3). This central result is given below in integral or differential form in Eqs. (53) or (66), respectively.

A. Integral equation of motion

We assume that the many-body Hamiltonian H has a form which is amenable to the Hubbard-Stratonovitch transformation. In particular, generalizing the discussion of the two-site Hubbard model, we write H as

$$H = H_0 - \frac{1}{2} \sum_{i=1}^n (H_i)^2, \quad (41)$$

where H_i , $i=0, n$, are one-body operators of the form

$$H_i = \underline{c}^\dagger * \underline{H}_i * \underline{c}. \quad (42)$$

Thus, H_0 is the one-body part of the many-body Hamiltonian and the $(H_i)^2$, $i=1, n$, give two-body interaction terms. As in the example above of the two-site Hubbard model, the many-body evolution operator $\exp(-\tau H)$ can now be expressed as the limit of the integral over Gaussian auxiliary fields x_{il} ,

$$\exp(-\tau H) = \lim_{m \rightarrow \infty} \int dG[\mathbf{x}] U_{\mathbf{x}}(\tau, 0), \quad (43)$$

where

$$U_{\mathbf{x}}(\tau, 0) = \prod_{l=1}^m \left[\exp(-\Delta\tau H_0) \prod_{i=1}^n \exp(-x_{il} H_i) \right] \quad (44)$$

is the Hubbard-Stratonovitch propagator for a particular choice $\{x_{il}\}$ of auxiliary fields which couple to the electrons through the fields H_i , and

$$dG[\mathbf{x}] = \prod_{l=1}^m \prod_{i=1}^n \frac{e^{-x_{il}^2/(2\Delta\tau)}}{\sqrt{2\pi\Delta\tau}} dx_{il} \quad (45)$$

is the Gaussian measure of the n fields on m time slices. We again emphasize that the advantage of this representation of the many-body propagator in the present context is that each Hubbard-Stratonovitch propagator involves one-body operators only and so maps the set of Slater determinants onto itself (i.e., the image of each Slater determinant under the Hubbard-Stratonovitch propagator is again a Slater determinant).

To obtain the integral representation, Eq. (40), of the propagated many-body wave function at time τ , we act on the integral representation of the wave function at initial time with the auxiliary-field representation of the propagator:

$$\begin{aligned} |\Phi(\tau)\rangle &= \int_{\mathbf{D}} f(\Psi; 0) \left[\int dG[\mathbf{x}] U_{\mathbf{x}}(\tau, 0) |\Psi\rangle \right] d\Psi \\ &= \int_{\mathbf{D}} f(\Psi; 0) \left[\int dG[\mathbf{x}] |\Psi_{\mathbf{x}}(\tau, 0)\rangle \right] d\Psi. \end{aligned} \quad (46)$$

(Here, and in the following discussion, we assume that the infinite time-slice limit $\lim_{m \rightarrow \infty}$ is taken, without explicitly writing it out.) We now want to transfer the τ dependence from the determinants $|\Psi\rangle$ onto the function $f(\Psi; \tau)$. This can be done by interchanging the order of integration over the manifold and over the auxiliary fields

$$\begin{aligned} \int_{\mathbf{D}} f(\Psi; 0) \left[\int dG[\mathbf{x}] |\Psi_{\mathbf{x}}(\tau, 0)\rangle \right] d\Psi \\ = \int dG[\mathbf{x}] \int_{\mathbf{D}} f(\Psi; 0) |\Psi_{\mathbf{x}}(\tau, 0)\rangle d\Psi, \end{aligned} \quad (47)$$

and changing the variable of integration over the manifold for each choice of the auxiliary fields

$$\begin{aligned} \int_{\mathbf{D}} f(\Psi; 0) |\Psi_{\mathbf{x}}(\tau, 0)\rangle d\Psi \\ = \int_{\mathbf{D}} f(\Psi; 0) [\langle \Psi_{\mathbf{x}}(\tau, 0) | \Psi_{\mathbf{x}}(\tau, 0) \rangle]^{1/2} |\Psi'\rangle \frac{d\Psi}{d\Psi'} d\Psi', \end{aligned} \quad (48)$$

where Ψ' is the image in \mathbf{D} of Ψ under propagation by the particular choice \mathbf{x} of auxiliary fields:

$$|\Psi'\rangle = [\langle \Psi_{\mathbf{x}}(\tau, 0) | \Psi_{\mathbf{x}}(\tau, 0) \rangle]^{-1/2} |\Psi_{\mathbf{x}}(\tau, 0)\rangle, \quad (49)$$

and

$$\frac{d\Psi}{d\Psi'} = J[\mathbf{x}; \Psi'] \quad (50)$$

is the inverse of the Jacobian of the transformation $\Psi \rightarrow \Psi'$ on \mathbf{D} . Conversely, Ψ is the image of Ψ' under the inverse flow $U_{\mathbf{x}}(0, \tau)$, where the backward propagator

$U_{\mathbf{x}}(0, \tau)$ is the inverse of the forward propagator $U_{\mathbf{x}}(\tau, 0)$ in Eq. (44). Thus, the integral representation of $|\Phi(\tau)\rangle$ can be written as

$$\begin{aligned} |\Phi(\tau)\rangle &= \int_{\mathbf{D}} \left[\int dG[\mathbf{x}] f(U_{\mathbf{x}}(0, \tau) \right. \\ &\quad \left. \times |\Psi'; 0\rangle W_{\mathbf{x}}[\tau; \Psi'] \right] |\Psi'\rangle d\Psi', \end{aligned} \quad (51)$$

where the weight function

$$W_{\mathbf{x}}[\tau; \Psi'] = J[\mathbf{x}; \Psi'] [\langle \Psi'_{\mathbf{x}}(0, \tau) | \Psi'_{\mathbf{x}}(0, \tau) \rangle]^{-1/2} \quad (52)$$

includes both the Jacobian of the inverse flow and the change in the normalization of $|\Psi'\rangle$ under the inverse propagation. We now have the integral representation of $|\Phi(\tau)\rangle$ written in a form where we can identify the correct form of $f(\Psi; \tau)$ as

$$f(\Psi; \tau) = \int dG[\mathbf{x}] f(U_{\mathbf{x}}(0, \tau) \Psi; 0) W_{\mathbf{x}}[\tau; \Psi]. \quad (53)$$

The value of $f(\Psi; \tau)$ is thus an average of the values of $f(\Psi; 0)$ at the endpoints of the random Gaussian backward flows $U_{\mathbf{x}}(0, \tau)$, each weighted by W to allow for re-normalization of the states by the propagator and spreading of the flow on the manifold \mathbf{D} .

B. Differential equation of motion

We will now work from this integral form for the evolution of the function $f(\Psi; \tau)$ to a differential equation for f on \mathbf{D} . To do so, we will examine how the function f behaves for very small τ . In that case, we may assume that there is only one "time slice" in the interval $[0, \tau]$ (i.e., $m = 1$ or $\Delta\tau = \tau$), and that the action of the different auxiliary fields can be treated separately from each other and from the one-body part H_0 . [This separation of the effects of the different fields is justified because their effects fail to commute only at $O(\Delta\tau^2)$.] The propagator for the i th field is then simply

$$U_x(\tau, 0) = \exp(-xH_i), \quad (54)$$

and x has a Gaussian distribution with zero mean and variance equal to τ . Considering the effect of this field alone we have that

$$f(\Psi; \tau) = \int_{-\infty}^{+\infty} f(U_x(0, \tau) \Psi; 0) W_x[\tau; \Psi] \frac{e^{-x^2/(2\tau)}}{\sqrt{2\pi\tau}} dx. \quad (55)$$

Let us consider the value of f at a particular point Ψ_0 on \mathbf{D} . The variable x parametrizes a curve on \mathbf{D} through Ψ_0 as follows:

$$|\Psi(x)\rangle = \exp(xH_i) |\Psi_0\rangle [\langle \Psi_0 | \exp(2xH_i) | \Psi_0 \rangle]^{-1/2}. \quad (56)$$

We define the weighting factor

$$w(x) = W_x[\tau; \Psi] = n(x) J(x), \quad (57)$$

where

$$n(x) = \langle \Psi_0 | \exp(2xH_i) | \Psi_0 \rangle^{-1/2} \quad (58)$$

accounts for the change in the normalization of states un-

der propagation and

$$J(x) = \frac{d\Psi(x)}{d\Psi_0}, \quad (59)$$

is the Jacobian of the inverse flow on \mathbf{D} . Note that $\Psi(x)$ and $w(x)$ do not depend directly on τ and that the τ dependence of f comes only from the Gaussian integration. The integral equation (55) for $f(\Psi_0; \tau)$ now takes the form

$$f(\Psi_0; \tau) = \int_{-\infty}^{+\infty} f(\Psi(x); 0) w(x) \frac{e^{-x^2/(2\tau)}}{\sqrt{2\pi\tau}} dx. \quad (60)$$

Expanding $f(\Psi(x); 0)w(x)$ in a power series about $x = 0$, we have that

$$f(\Psi_0; \tau) = \int_{-\infty}^{+\infty} \left[f(\Psi_0; 0)w(0) + \frac{\partial f w}{\partial x} x + \frac{1}{2} \frac{\partial^2 f w}{\partial x^2} x^2 + \dots \right] \frac{e^{-x^2/(2\tau)}}{\sqrt{2\pi\tau}} dx. \quad (61)$$

Only even powers of x contribute to the Gaussian-weighted integral and x^{2n} contributes a term proportional to τ^n . Also, note that $w(0) = 1$. Thus,

$$f(\Psi_0; \tau) - f(\Psi_0; 0) = \frac{1}{2} \frac{\partial^2 f w}{\partial x^2} \tau + \mathcal{O}(\tau^2) \\ = \left[\frac{1}{2} \frac{\partial^2 f}{\partial x^2} + \frac{\partial f}{\partial x} \frac{\partial w}{\partial x} + \frac{1}{2} \frac{\partial^2 w}{\partial x^2} f(\Psi_0; 0) \right] \tau + \mathcal{O}(\tau^2). \quad (62)$$

Each auxiliary field contributes in a similar way to the change in f over the short interval $[0, \tau]$. The contribution of the one-body term H_0 is somewhat different since it involves no integration over auxiliary fields. Considering that field alone, the inverse evolution of the state $|\Psi_0\rangle$ is just

$$|\Psi(x)\rangle = \exp(xH_0) |\Psi_0\rangle, \quad (63)$$

where x is set equal to τ . The variable x is no longer integrated over. With the functions of x now defined as before, except with H_0 replacing H_i , the change in f over the interval $[0, \tau]$ due to this term is given by

$$f(\Psi_0; \tau) - f(\Psi_0; 0) = \left[\frac{\partial f}{\partial x} + \frac{\partial w}{\partial x} f(\Psi_0; 0) \right] \tau + \mathcal{O}(\tau^2). \quad (64)$$

Adding the contributions of all fields to the change in f over the interval $[0, \tau]$ to first order in τ , we get the partial derivative of f with respect to τ as

$$\frac{\partial f(\Psi_0; \tau)}{\partial \tau} = \frac{\partial f}{\partial x_0} + \frac{\partial w}{\partial x_0} f(\Psi_0; \tau) \\ + \sum_{i=1}^n \left[\frac{1}{2} \frac{\partial^2 f}{\partial x_i^2} + \frac{\partial f}{\partial x_i} \frac{\partial w}{\partial x_i} + \frac{1}{2} \frac{\partial^2 w}{\partial x_i^2} f(\Psi_0; \tau) \right]. \quad (65)$$

As shown in the Appendix, by a change of coordinates from the x_i to the coordinates ε_{ij} defined in Sec. III, this equation can be transformed into a differential equation for $f(\Psi; \tau)$ in the intrinsic coordinates ε_{ij} on \mathbf{D} . The equation is of the form

$$\frac{\partial f}{\partial \tau} = \frac{1}{2} D(\Psi) f + [\nabla_{\Psi} V_1(\Psi)] \nabla_{\Psi} f - V_2(\Psi) f, \quad (66)$$

where $D(\Psi)$ gives the diffusion terms

$$D(\Psi) f = \sum_{i=1}^n \langle \underline{u}_k | H_i | \underline{u}_j \rangle \langle \underline{u}_m | H_i | \underline{u}_l \rangle \frac{\partial^2 f}{\partial \varepsilon_{jk} \partial \varepsilon_{lm}}, \quad (67)$$

where the single-particle wave functions \underline{u}_j are defined as in Eq. (29). The gradient (or drift) terms are governed by the function

$$V_1(\Psi) = \frac{1}{2} \left\{ \langle \Psi | H_0 | \Psi \rangle + \sum_{i=1}^n [M \text{Tr} \underline{H}_i - \left\{ \frac{N+1}{2} \right\} \langle \Psi | H_i | \Psi \rangle] \times \langle \Psi | H_i | \Psi \rangle \right\}, \quad (68)$$

where $\text{Tr} \underline{H}_i$ is the trace of H_i as a one-body operator. (As before, M is the number of particles and N is the dimension of the single-particle Hilbert space.) The branching (or decay) terms are proportional to the function

$$V_2(\Psi) = -M \text{Tr} \underline{H}_0 + (N+1) \langle \Psi | H_0 | \Psi \rangle \\ - \frac{1}{2} \sum_{i=1}^n \left\{ [M \text{Tr} \underline{H}_i - (N+1) \langle \Psi | H_i | \Psi \rangle]^2 - 2(N+1) [\langle \Psi | H_i^2 | \Psi \rangle - (\langle \Psi | H_i | \Psi \rangle)^2] \right\}. \quad (69)$$

At this point we have essentially integrated out again the auxiliary fields we introduced initially with the Hubbard-Stratonovitch transformation and it might appear that the evolution of the function $f(\Psi; \tau)$ is independent of the particular transformation used. However, the mapping of the many-body problem onto the diffusion equation (66) on \mathbf{D} depends crucially on the Hubbard-Stratonovitch transformation. The operators H_i , through which the auxiliary fields couple to the electrons, appear explicitly in the coefficients of Eq. (66), as given in Eqs. (67)–(69). Different Hubbard-Stratonovitch transformations of the original many-body problem will lead to different diffusion equations on \mathbf{D} even though they must give the same evolution of the many-body state $|\Phi(\tau)\rangle$ defined from f in Eq. (40). This apparent paradox is easily resolved when one recalls that the set of *all* Slater determinants is a vastly overcomplete basis for the many-particle Hilbert space. An infinity of different weight functions $f(\Psi; \tau)$ can give the same many-body state via Eq. (40).

Finally, we note that the lack of correlation between

different auxiliary fields was crucial to the derivation of diffusive behavior of the states. In a situation where the auxiliary fields have a genuine physical dynamics,²⁹ as they do in a coupled electron-phonon system, where the phonon fields take the role of the auxiliary fields, one cannot apply the same arguments. In the simulation of the auxiliary fields using importance sampling of the quantity

$$|\langle \Psi_t | U_x(\tau, 0) | \Psi_t \rangle| ,$$

the magnitude of this quantity induces strong correlations in the auxiliary fields which are sampled. However, in the original Gaussian measure, defined in Eq. (45), there is no intrinsic correlation between different fields. The dynamics of the fields induced by importance sampling is the subject of a separate investigation.²⁷

V. DISCUSSION

We emphasize that nothing *extra* has been introduced beyond the Hubbard-Stratonovitch transformation in obtaining the diffusion equation (66). The distribution function $f(\Psi; \tau)$ (and its diffusive behavior) was already implicitly contained in the auxiliary-field projection approach. We should also point out that the diffusion equation (66) only depends on the form of the many-body Hamiltonian in Eq. (41), and is not restricted to the Hubbard model. Although Eq. (66) is formally simple—a diffusion equation with drift and branching terms—the exact solution is by no means easy to envisage and a number of subtle points can affect its behavior. However, the diffusion form in which the evolution of the many-body state is now cast allows us to understand qualitatively which determinants contribute to the representation of the ground state in an important way. In particular, regions of \mathbf{D} where the “potentials” V_1 and V_2 are high will be avoided since (returning to the random-walk view of equations of this type) the drift terms will force walkers away from regions where V_1 is high and branching will cause annihilation of walkers in regions where V_2 is high,^{6,11}. When the interaction terms are small, both of these functions are dominated by the noninteracting system energy $\langle \Psi | H_0 | \Psi \rangle$, so that the noninteracting ground state predominates and the mixture of other states is small. The interaction terms favor regions where the energies $\langle \Psi | H_i | \Psi \rangle^2$ are large. In the case of the Hubbard model, where $H_i = n_{i\uparrow} - n_{i\downarrow}$, this can be achieved by ensuring that the Slater determinant maximizes the magnetization on each site, clearly giving a tendency towards ferromagnetism or antiferromagnetism.²⁶

Thus, the potentials V_1 and V_2 reflect some of the behavior one expects intuitively from the problem and give rise to a representation of the ground state which is concentrated near the mean-field solutions. The form of V_1 and V_2 are certainly sufficiently complicated that a precise connection between their minima and the mean-field solutions is not obvious. In the two-site Hubbard model example of Sec. II, the maximum of the asymptotic distribution of $f(\Psi; \beta)$ does not, in fact, occur exactly at the mean-field solution but is slightly displaced from it. However, the general physical characteristics of the mean-field solution are similar to those of the state Ψ at

which f is a maximum; both follow a comparable transition from delocalized, independent-electron behavior to a localized, Heitler-London-like state as the interaction parameter U increases. In simulations of the auxiliary-field method for cases up to 4×4 sites of the square-lattice Hubbard model, we have found the same very strong connection between the mean-field solutions and the regions where the asymptotic distribution of $f(\Psi; \beta)$ is concentrated. How well this connection is obeyed in the general case of the Hubbard-Stratonovitch approach is probably some measure of how “appropriate” a particular choice of the Hubbard-Stratonovitch transformation is for the physics of the many-body problem at hand.

We now turn to the issue of the exponential decay of the average sign $\sigma(\beta)$ defined in Eqs. (7) and (8) for the auxiliary-field method. It is clear that inversion of the manifold \mathbf{D} , defined by $|\Psi\rangle \rightarrow -|\Psi\rangle$, commutes with the diffusion equation operator on \mathbf{D} . It follows that the eigenfunctions of the differential equation can be classified by parity; a function f on \mathbf{D} is even if $f(\Psi) = f(-\Psi)$ and odd if $f(\Psi) = -f(-\Psi)$. Since the diffusion equation propagator defined in Eq. (53) always maps positive functions into positive functions, the eigenfunction with the highest eigenvalue in general will be non-negative everywhere since this eigenfunction will dominate at large times. In fact, it will be strictly positive everywhere if the diffusion process is ergodic on \mathbf{D} . Thus, in general, the eigenfunction with the highest eigenvalue has even parity. [Note that the *highest* eigenvalue of a diffusion propagator $\exp(-\tau H)$ is the most slowly decaying and corresponds to the *lowest* eigenvalue of the Hamiltonian H .]

However, any even-parity function f^+ gives a zero many-body state

$$\int_{\mathbf{D}} f^+(\Psi) |\Psi\rangle d\Psi = 0 , \quad (70)$$

and so its eigenvalue does not correspond to an eigenvalue of the many-body operator. Only odd-parity functions f^- can give rise to nonzero many-body states. Considering the scheme of Sorella *et al.*,^{8,9} we see that the usual “partition function”

$$Z(\beta) = \int_{\mathbf{D}} f(\Psi; \beta) \langle \Psi_t | \Psi \rangle d\Psi , \quad (71)$$

where $f(\Psi; 0) = \delta(\Psi - \Psi_t)$, couples only to the odd-parity functions, while their unsigned partition function

$$Z^\dagger(\beta) = \int_{\mathbf{D}} f(\Psi; \beta) |\langle \Psi_t | \Psi \rangle| d\Psi \quad (72)$$

couples only to the even-parity functions. Thus, the average sign $\sigma(\beta) = Z(\beta) / Z^\dagger(\beta)$ will decay exponentially as $\beta \rightarrow \infty$ with an exponent equal to the difference between the highest even-parity eigenvalue and the highest odd-parity eigenvalue. In exceptional circumstances this difference may be zero [see the remarks about “pathological” behavior of Eq. (66) below], in which case the average sign tends to a constant. These results are in accord with assertions of Sorella *et al.*⁹ that the sign either tends to a constant or goes exponentially to zero.

The sign decay in the grand canonical approach can be understood in the same context. At large β , the most probable fermion number M dominates the grand canoni-

cal average. Decomposing the determinant the operator $I + U_x(\beta, 0)$ into contributions from propagating individual M -fermion trial states,¹⁸ we realize that each term in the trace simply corresponds to a different initial condition $f(\Psi; 0)$ for the same diffusion problem on the M -fermion manifold of Slater determinants. The same functions f^+ and f^- thus dominate all the contributions to the (grand) canonical determinant at large β , explaining the comparable decay rates of $\sigma(\beta)$ observed for both grand canonical and projection approaches.^{10,18}

The connection of regions which are parity images of each other by diffusion paths is the crucial factor determining the splitting of the odd and even eigenvalues. If it is possible to diffuse from Ψ to $-\Psi$ for a point Ψ where the asymptotic distribution of $f(\Psi; \beta)$ is not zero, then the difference between the highest even-parity eigenvalue and the highest odd-parity eigenvalue must be nonzero. The greater the “ease” of diffusion (i.e., the shorter the average transit time from Ψ to $-\Psi$), the greater the splitting of the eigenvalues and the more rapid the decay of the average sign. On the other hand, in the exceptional case when $-\Psi$ cannot be reached by diffusion from Ψ , then the odd- and even-parity eigenvalues are degenerate and the sign tends to a constant as $\beta \rightarrow \infty$.

For the weakly interacting system the potentials $V_1(\Psi)$ and $V_2(\Psi)$ are dominated by $\langle \Psi | H_0 | \Psi \rangle$. If Ψ_0 is the noninteracting ground state, the minimum barrier in the function $\langle \Psi | H_0 | \Psi \rangle$ between Ψ_0 and $-\Psi_0$ equals the gap to the first excited state of the noninteracting system. Thus, if the noninteracting Hamiltonian has a degenerate ground state (and so is metallic), there will be no barrier to diffusion between Ψ_0 and $-\Psi_0$ to a first approximation. This is why closed-shell systems (where the noninteracting ground state is nondegenerate), in general, have a much slower rate of decay of the average sign than open-shell systems (where the noninteracting ground state is degenerate). When the interaction terms are stronger, we have found that the mean-field solutions take on the same qualitative role as the noninteracting ground state has for weak interaction, and the ease of diffusion between different equivalent mean-field solutions typically determines the rate of decay of the average sign $\sigma(\beta)$.

This diffusion picture of the auxiliary-field method reveals a common formal origin of its “sign problem” and that of the Green’s-function Monte Carlo method. In both cases, one is dealing with a diffusion-type problem. The asymptotic solution of this diffusion, to which numerical simulations will naturally tend, is everywhere positive. In each approach this nodeless solution belongs to the identity irreducible representation of some symmetry group of the diffusion operator. However, the solution which one requires for the *physical* problem belongs to a different representation of this symmetry group—a representation which must be negative in some regions. In the Green’s-function Monte Carlo, the symmetry involved is the exchange of particles, under which fermion wave functions are required to be antisymmetric. In the auxiliary-field projection method, the symmetry involved is the parity operator, $\Psi \rightarrow -\Psi$, under which physically relevant solutions of the diffusion problem must be odd.

Moreover, the diffusion picture of the auxiliary-field approach gives us a clear understanding of why the approximation of using the unsigned partition function $Z^\dagger(\beta)$ yields a reasonable approximation for *all* physical properties of the system (not just the energy) in cases where the decay of the average sign is slow. If Ψ_t is in one of the regions where the drift and branching potentials V_1 and V_2 are low, and there are substantial barriers of the functions V_1 and V_2 inhibiting diffusion from Ψ_t to $-\Psi_t$, then we could solve the diffusion equation approximately in regions where V_1 and V_2 are low. These regions are dominant in the slowly decaying eigenfunctions of the diffusion operator. The slowest decaying even- and odd-parity wave functions can then be constructed approximately as even and odd linear combinations, respectively, of the slowest decaying approximate solutions where V_1 and V_2 are low. Then

$$\int_{\mathbf{D}} f^+(\Psi) \text{sgn}(\langle \Psi_t | \Psi \rangle) |\Psi\rangle d\Psi \approx \int_{\mathbf{D}} f^-(\Psi) |\Psi\rangle d\Psi, \quad (73)$$

and so one obtains approximately the correct many-body ground state [corresponding to $f^-(\Psi)$] in using the many-body state corresponding to $f^+(\Psi) \text{sgn}(\langle \Psi_t | \Psi \rangle)$, which is qualitatively similar to using $Z^\dagger(\beta)$ in calculating all physical quantities.³⁰

We close this discussion with some remarks about the kinds of “pathological” behavior, some of which the diffusion equation (66) displays in general, and some in exceptional cases. A point which complicates the analysis of the diffusion equation (66), in general, is the fact that the equation is degenerate in the sense that the diffusion at any point does not act in all directions of the manifold. There are $M(N-M)$ directions in the manifold but there are only n auxiliary fields, and so, at most, n linearly independent directions of diffusion on \mathbf{D} at any given point. Thus, the rank of the matrix of diffusion coefficients defined in Eq. (67) is at most n . In the two-site Hubbard model example, there is only one effective auxiliary field; viz., that which couples to $(n_{1\uparrow} - n_{2\uparrow}) - (n_{1\downarrow} - n_{2\downarrow})$. The other independent field couples to the total magnetization $(n_{1\uparrow} + n_{2\uparrow}) - (n_{1\downarrow} + n_{2\downarrow})$, a conserved quantity which gives rise to no real dynamics on the manifold \mathbf{D} .

Furthermore, the manifold might be divided into separate regions by a surface where all normal components of diffusion are zero. This will give rise to solutions of the diffusion problem being confined entirely to one of the separate regions. Again, in the two-site Hubbard model (see Fig. 1), the θ_1 and θ_2 axes form such surfaces, as do the lines $\theta_1 - \theta_2 = \pm\pi/2$ (i.e., the submanifold of states with particle-hole symmetry). Thus, if the initial trial state Ψ_t is within the triangle with vertices $(0,0)$, $(\pi/2,0)$, $(0,\pi/2)$, the final distribution will be entirely contained within that triangle also. In this case the odd and even eigenfunctions of the diffusion will be degenerate and the average sign will tend to a constant as $\beta \rightarrow \infty$. However, we must say that, although this circumstance is highly advantageous from the point of view of numerical auxiliary-field simulations, it is very much the exception rather than the rule. Moreover, we do not know any way that the Hubbard-Stratonovitch transfor-

mation could be set up in advance for the general problem in order to achieve this nonergodic behavior of the diffusion and strict degeneracy of the odd and even eigenfunctions.

The collapse of the distribution f onto the line of states with particle-hole symmetry in Fig. 2 is quite striking. In general, it may happen that there is a submanifold of \mathbf{D} which is stable in the sense that the diffusion and drift directions for points on the manifold are always parallel to the manifold and points near the manifold tend to drift onto it. In that case, points which start on the manifold never diffuse or drift off it and the diffusion problem can be confined and solved on that manifold alone. This occurs, for example, in the half-filled Hubbard model, where the states which have particle-hole symmetry^{26,27} form such a stable manifold.

The lack of a one-to-one correspondence between the eigenvalues of the diffusion operator and those of the original many-body operator is a consequence of the overcompleteness of the representation which we use of the many-body states in terms of *all* Slater determinants. Indeed, although the many-body Hamiltonian has a finite number of eigenvalues, the diffusion operator may have an infinite number. Mathematically, the diffusion operator is not very tractable since it is not self-adjoint (the drift terms cause it to be non-self-adjoint). However, it is a differential operator on a compact manifold \mathbf{D} and so one may expect it to be reasonably well behaved and many of its properties to be intuitively apparent.

VI. CONCLUSIONS

In conclusion, we have developed a view of the auxiliary-field projection approach in terms of a differential equation with diffusion, drift, and branching terms on the manifold of normalized Slater determinants. This view offers substantial insight into the behavior of the method, allowing a qualitative understanding of the states dominant in representing the ground state. It also provides a common formal view of the continuum Green's-function or diffusion and the auxiliary-field projection methods. It demonstrates the exponential decay of the average sign in the auxiliary-field approach to be a consequence of the general property of diffusion equations that they have nodeless ground states. We have illustrated the dynamical behavior of resulting representation of many-body states in a simple two-site Hubbard model. As topics for future study, the view offers interesting possibilities for approximating ground-state properties from approximate solutions of the diffusion equation in regions of the manifold of Slater determinants where the drift and branching potentials are low. It also suggests corrections to the Sorella approximation of neglecting minus signs in the action might be calculated using approximate "barrier penetration rate" methods familiar in other contexts.

APPENDIX

In this appendix, we transform the differential equation (65) for $f(\Psi; \tau)$ involving the auxiliary-field derivatives into a form in terms of derivatives with respect to the

basic coordinates of the manifold \mathbf{D} , i.e., the local orthonormal coordinates ε_{ij} at each point. For simplicity, we will assume that all wave functions involved in the problem are real and make no distinction between a quantity like $\langle \Psi | \Psi' \rangle$ and its complex conjugate $\langle \Psi' | \Psi \rangle$. This is a justifiable approach when all the auxiliary fields are real—as they are in the problem as we have presented it.

The derivative of the flow $\exp(xH_i)$ on \mathbf{D} is given by the component of $H_i | \Psi \rangle$ along the manifold (i.e., normal to $| \Psi \rangle$ itself). Thus,

$$\frac{d\Psi}{dx} = H_i | \Psi \rangle - | \Psi \rangle \langle \Psi | H_i | \Psi \rangle \equiv TH_i \Psi. \quad (\text{A1})$$

This serves to define the action of T , which takes the component tangential to \mathbf{D} of any vector associated with the point Ψ of \mathbf{D} . The derivative with respect to \underline{x} of any function f on \mathbf{D} is then given by

$$\frac{\partial f}{\partial \underline{x}} \equiv (TH_i \Psi) \cdot \nabla_{\Psi} f. \quad (\text{A2})$$

The component of the flow derivative $TH_i \Psi$ along the local coordinate axis $\hat{\varepsilon}_{lm}$ of the manifold is equal to the matrix element of H_i for that particle-hole excitation:

$$\hat{\varepsilon}_{lm} \cdot (TH_i \Psi) = \langle \hat{\varepsilon}_{lm} | H_i | \Psi \rangle = \langle \underline{u}_m | H_i | \underline{u}_l \rangle. \quad (\text{A3})$$

Also note that the flow derivative $TH_i \Psi$ along the manifold is half the gradient of the expectation value of H_i in the state $| \Psi \rangle$:

$$TH_i \Psi = \frac{1}{2} \nabla_{\Psi} \langle \Psi | H_i | \Psi \rangle. \quad (\text{A4})$$

The logarithmic derivative of the inverse normalization factor $n(x)$ under propagation by $\exp(xH_i)$ is given by

$$\frac{1}{n} \frac{\partial n}{\partial x} = - \langle \Psi(x) | H_i | \Psi(x) \rangle, \quad (\text{A5})$$

and the logarithmic derivative of the Jacobian $J(x)$ of the mapping $\Psi_0 \rightarrow \Psi(x)$ on \mathbf{D} is equal to the divergence of the flow derivative

$$\frac{1}{J} \frac{\partial J}{\partial x} = \nabla_{\Psi} \cdot (TH_i \Psi). \quad (\text{A6})$$

Making use of the basic definition of $TH_i \Psi$ in Eq. (A1) to calculate its rate of change along the manifold in the direction $\hat{\varepsilon}_{lm}$, it is straightforward to show that

$$\begin{aligned} \hat{\varepsilon}_{lm} \frac{\partial TH_i \Psi}{\partial \varepsilon_{lm}} &= \langle \hat{\varepsilon}_{lm} | H_i | \hat{\varepsilon}_{lm} \rangle - \langle \Psi | H_i | \Psi \rangle \\ &= \langle \underline{u}_m | H_i | \underline{u}_m \rangle - \langle \underline{u}_l | H_i | \underline{u}_l \rangle. \end{aligned} \quad (\text{A7})$$

Summing over all orthogonal directions in the manifold gives³¹

$$\begin{aligned} \frac{1}{J} \frac{\partial J}{\partial x} &= \sum_{l=1}^M \sum_{m=M+1}^N (\langle \underline{u}_m | H_i | \underline{u}_m \rangle - \langle \underline{u}_l | H_i | \underline{u}_l \rangle) \\ &= M \text{Tr} \underline{H}_i - N \langle \Psi | H_i | \Psi \rangle, \end{aligned} \quad (\text{A8})$$

where $\text{Tr} \underline{H}_i$ is the trace of H_i as a one-body operator. Putting together the derivatives for $n(x)$ and $J(x)$ gives

us the derivative of their product $w(x)$:

$$\frac{1}{2} \frac{\partial w}{\partial x} = \frac{1}{n} \frac{\partial n}{\partial x} + \frac{1}{J} \frac{\partial J}{\partial x} = M \operatorname{Tr} \underline{H}_i - (N+1) \langle \Psi | \underline{H} | \Psi \rangle. \quad (\text{A9})$$

The contribution of $(\partial w / \partial x)(\partial f / \partial x)$ to the gradient (or drift) term in the differential equation (66) for f is

$$\begin{aligned} \frac{\partial w}{\partial x} \frac{\partial f}{\partial x} &= [M \operatorname{Tr} \underline{H}_i - (N+1) \langle \Psi | H_i | \Psi \rangle] (TH_i \Psi) \cdot \nabla_{\Psi} f \\ &= \frac{1}{2} \left\{ \nabla_{\Psi} \left[M \operatorname{Tr} \underline{H}_i - \left(\frac{N+1}{2} \right) \langle \Psi | H_i | \Psi \rangle \right] \right. \\ &\quad \left. \times \langle \Psi | H_i | \Psi \rangle \right\} \nabla_{\Psi} f. \end{aligned} \quad (\text{A10})$$

Turning now to the coefficient of f in Eq. (66) coming from $\frac{1}{2}(\partial^2 w) / \partial x^2$ in Eq. (65), we note that

$$\frac{1}{w} \frac{\partial^2 w}{\partial x^2} = \left[\frac{1}{w} \frac{\partial w}{\partial x} \right]^2 + \frac{\partial}{\partial x} \left[\frac{1}{w} \frac{\partial w}{\partial x} \right], \quad (\text{A11})$$

and that

$$\begin{aligned} \frac{\partial}{\partial x} \left[\frac{1}{w} \frac{\partial w}{\partial x} \right] &= (TH_i \Psi) \cdot \nabla_{\Psi} [M \operatorname{Tr} \underline{H}_i - (N+1) \langle \Psi | H_i | \Psi \rangle] \\ &= -(N+1) (TH_i \Psi) \cdot \nabla_{\Psi} \langle \Psi | H_i | \Psi \rangle \\ &= -2(N+1) (TH_i \Psi) \cdot (TH_i \Psi) \\ &= -2(N+1) (\langle \Psi | H_i | \Psi \rangle - \langle \Psi | H_i | \Psi \rangle \langle \Psi | H_i | \Psi \rangle) \\ &= -2(N+1) [\langle \Psi | H_i^2 | \Psi \rangle - (\langle \Psi | H_i | \Psi \rangle)^2]. \end{aligned} \quad (\text{A12})$$

The branching term (i.e., the term multiplying f) in the differential equation (61) for f is then given by

$$\begin{aligned} \frac{1}{2} \frac{\partial^2 w}{\partial x^2} f &= \frac{1}{2} \left\{ [M \operatorname{Tr} H_i - (N+1) \langle \Psi | H_i | \Psi \rangle]^2 \right. \\ &\quad - 2(N+1) [\langle \Psi | H_i^2 | \Psi \rangle \\ &\quad \left. - (\langle \Psi | H_i | \Psi \rangle)^2] \right\} f. \end{aligned} \quad (\text{A13})$$

The second derivative of f with respect to x on Eq. (65) can be expanded to give drift and diffusion terms in local coordinates:

$$\begin{aligned} \frac{1}{2} \frac{\partial^2 f}{\partial x^2} &= \frac{1}{2} (TH_i \Psi) \cdot \nabla_{\Psi} [(TH_i \Psi) \cdot \nabla_{\Psi} f] \\ &= \frac{1}{2} [(TH_i \Psi) \cdot \nabla_{\Psi} TH_i \Psi] \nabla_{\Psi} f \\ &\quad + \frac{1}{2} \sum_{j,l=1}^M \sum_{k,m=M+1}^N \langle \underline{u}_k | H_i | \underline{u}_j \rangle \langle \underline{u}_m | H_i | \underline{u}_l \rangle \\ &\quad \times \frac{\partial^2 f}{\partial \epsilon_{jk} \partial \epsilon_{lm}}. \end{aligned} \quad (\text{A14})$$

The first term on the right-hand side contributes to the drift term $\nabla_{\Psi} f$ in the differential equation for f and the second sum of terms gives a diffusion contribution. The drift term can be written as

$$\begin{aligned} \frac{1}{2} [(TH_i \Psi) \cdot \nabla_{\Psi} TH_i \Psi] \nabla_{\Psi} f &= \frac{1}{4} [\nabla_{\Psi} (TH_i \Psi)^2] \nabla_{\Psi} f \\ &= \frac{1}{4} [\nabla_{\Psi} (\langle \Psi | H_i^2 | \Psi \rangle \\ &\quad - \langle \Psi | H_i | \Psi \rangle^2)] \nabla_{\Psi} f. \end{aligned} \quad (\text{A15})$$

The one-body potential H_0 contributes drift and branching terms but no diffusion terms to the differential equation. The drift term is

$$\frac{\partial f}{\partial x_0} = (TH_0 \Psi) \cdot \nabla_{\Psi} f = \frac{1}{2} (\nabla_{\Psi} \langle \Psi | H_0 | \Psi \rangle) \nabla_{\Psi} f \quad (\text{A16})$$

and the branching term is

$$\begin{aligned} \frac{\partial w}{\partial x_0} f &= [\nabla_{\Psi} \cdot (TH_0 \Psi) - \langle \Psi | H_0 | \Psi \rangle] f \\ &= [M \operatorname{Tr} \underline{H}_0 - (N+1) \langle \Psi | H_0 | \Psi \rangle] f. \end{aligned} \quad (\text{A17})$$

- ¹N. Metropolis and S. Ulam, *J. Am. Stat. Assoc.* **44**, 335 (1949).
²M. H. Kalos, D. Levesque, and L. Verlet, *Phys. Rev. A* **9**, 2178 (1974).
³D. M. Ceperley and B. J. Alder, *Phys. Rev. Lett.* **45**, 566 (1980).
⁴P. J. Reynolds, R. N. Barnett, B. L. Hammond, and W. A. Lester, *J. Stat. Phys.* **43**, 1017 (1986).
⁵D. M. Ceperley and B. J. Alder, *Phys. Rev. B* **36**, 2092 (1987).
⁶For a recent elementary review of the Green's-function Monte Carlo method, see M. H. Kalos and P. A. Whitlock, *Monte Carlo Methods* (Wiley, New York, 1986), Vol. 1, Chap. 8.
⁷G. Sugiyama and S. E. Koonin, *Ann. Phys. (N.Y.)* **168**, 1 (1986).
⁸S. Sorella, E. Tosatti, S. Baroni, R. Car, and M. Parrinello, *Int. J. Mod. Phys. B* **1**, 993 (1988).
⁹S. Sorella, S. Baroni, R. Car, and M. Parrinello, *Europhys.*

- Lett.* **8**, 663 (1989).
¹⁰E. Y. Loh, Jr., J. E. Gubernatis, R. T. Scalettar, S. R. White, D. J. Scalapino, and R. L. Sugar, *Phys. Rev. B* **41**, 9301 (1990).
¹¹For a general review of stochastic methods in many-body problems, see J. W. Negele and H. Orland, *Quantum Many-Particle Systems* (Addison-Wesley, Redwood City, California, 1988), Chap. 8.
¹²M. A. Lee, K. A. Motakabbir, and K. E. Schmidt, *Phys. Rev. Lett.* **53**, 1191 (1984).
¹³J. Carlson, *Phys. Rev. B* **40**, 846 (1989).
¹⁴N. Trivedi and D. M. Ceperley, *Phys. Rev. B* **40**, 2739 (1989).
¹⁵R. L. Stratonovitch, *Dokl. Akad. Nauk. SSSR* **115**, 1097 (1957) [*Sov. Phys. Dokl.* **2**, 416 (1957)].
¹⁶J. Hubbard, *Phys. Rev. Lett.* **3**, 77 (1959).
¹⁷S. R. White, D. J. Scalapino, R. L. Sugar, E. Y. Loh, J. E.

- Gubernatis, and R. T. Scalettar, Phys. Rev. B **40**, 506 (1989), and references therein.
- ¹⁸D. R. Hamann and S. Fahy, Phys. Rev. B **41**, 11 352 (1990).
- ¹⁹R. Courant, K. Friedrichs, and H. Lewy, Math. Ann. **100**, 32 (1928).
- ²⁰A. Parola, S. Sorella, S. Baroni, R. Car, and M. Parrinello, and E. Tosatti, Physica C **162-164**, 771 (1989).
- ²¹K. E. Schmidt and M. H. Kalos, in *Applications of the Monte Carlo Method in Statistical Physics*, 2nd ed., edited by K. Binder (Springer, Berlin, 1987), p. 125.
- ²²J. Hubbard, Proc. R. Soc. London, Ser. A **276**, 238 (1963).
- ²³S. Q. Wang, W. E. Evenson, and J. R. Schrieffer, Phys. Rev. Lett. **23**, 92 (1969).
- ²⁴D. R. Hamann, Phys. Rev. Lett. **23**, 95 (1969); Phys. Rev. B **2**, 1373 (1970).
- ²⁵H. F. Trotter, Proc. Am. Math. Soc. **10**, 545 (1959); M. Suzuki, Commun. Math. Phys. **51**, 183 (1976).
- ²⁶J. E. Hirsch, Phys. Rev. B **31**, 4403 (1985).
- ²⁷S. Fahy and D. R. Hamann (unpublished).
- ²⁸The sampling of points shown here for each value of τ was generated by Monte Carlo sampling of the auxiliary fields \mathbf{x} using the importance function $|U_{\mathbf{x}}(\tau, 0)|\psi_i\rangle|$. The points shown correspond to the resulting propagated states $U_{\mathbf{x}}(\tau, 0)|\Psi_i\rangle$.
- ²⁹R. Blankenbecler, D. J. Scalapino, and R. L. Sugar, Phys. Rev. D **24**, 2278 (1981).
- ³⁰However, we note that the approach of Refs. 8 and 9 to the calculation of a physical quantity is not exactly equivalent to calculating the expectation value of the quantity for the many-body wave function defined in Eq. (73).
- ³¹This result does not apply if the dynamics and the integration measure $d\Psi$ are restricted to a submanifold of all the normalized Slater determinants. In our discussion of the two-site Hubbard model, for example, it would have to be appropriately modified since one does not sum over manifold directions corresponding to *all* particle-hole excitations, but only those that do not involve spin flips.